AIRCRAFT INTERIOR NOISE REDUCTION BY ALTERNATE RESONANCE TUNING

PROGRESS REPORT FOR THE PERIOD ENDING JUNE, 1990

NASA RESEARCH GRANT NO. NAG-1-722

Prepared for:

Structural Acoustics Branch
NASA Langley Research Center

Prepared by:

Dr. Donald B. Bliss
James A. Gottwald
Ramakrishna Srinivasan
Mark B. Gustaveson

Department of Mechanical Engineering
and Materials Science
Duke University
Durham, North Carolina 27706

AUGUST 1990

SECTION 1. INTRODUCTION

Existing interior noise reduction techniques for aircraft fuselages perform reasonably well at higher frequencies, but are inadequate at lower frequencies, particularly with respect to the low blade passage harmonics with high forcing levels found in propeller aircraft. A method is being studied which considers aircraft fuselages lined with panels alternately tuned to frequencies above and below the frequency that must be attenuated. Adjacent panels would oscillate at equal amplitude, to give equal source strength, but with opposite phase. Provided these adjacent panels are acoustically compact, the resulting cancellation causes the interior acoustic modes to become cutoff, and therefore be non-propagating and evanescent. This interior noise reduction method, called *Alternate Resonance Tuning* (ART), is currently being investigated both theoretically and experimentally. This new concept has potential application to reducing interior noise due to the propellers in advanced turboprop aircraft as well as for existing aircraft configurations.

The ART technique is a procedure intended to reduce low frequency noise within an aircraft fuselage. A fuselage wall could be constructed of, or lined with, a series of special panels which would allow the designer to control the wave number spectrum of the wall motion, thus controlling the interior sound field. By judicious tuning of the structural response of individual panels, wavelengths in the fuselage wall can be reduced to the order of the panel size, thus causing low frequency interior acoustic modes to be cutoff provided these panels are sufficiently small. By cutting off the acoustic modes in this manner, a significant reduction of interior noise at the propeller blade passage harmonics should be achieved.

Current noise control treatments have already demonstrated that the mass and stiffness of individual fuselage panels can be altered. It seems reasonable, therefore, that panel resonance frequencies can be manipulated to achieve the ART effect.

Application of this concept might involve the modification of existing structural panels or development of a new design for fuselage interior trim panels. Although complete acoustic cutoff will not be achievable in practice, an approximate cancellation should still substantially reduce the interior noise levels at the particular frequency of interest. It is important to note that the ART method utilizes the flexibility and dynamic behavior of the structure to good advantage, although these properties are not normally beneficial in noise control.

This progress report summarizes the work carried out at Duke University during the seventh six month period of a contract supported by the Structural Acoustics Branch at NASA Langley. Considerable progress has been made both theoretically and experimentally as described in the following sections. It is important to note that all of the work carried out so far indicates the ART concept is indeed capable of achieving a significant reduction in the sound transmission through flexible walls.

SECTION 2.1 PRESENTATIONS TO DATE

D. B. Bliss, J. A. Gottwald, and R. Srinivasan, "Interior Noise Reduction by Alternate Resonance Tuning (ART)", Acoustical Society of America North Carolina Regional Chapter Spring Meeting Program, North Carolina State University, Raleigh, NC, March 22-23, 1990 (presented by D. B. Bliss).

D. B. Bliss, "Analysis of Acoustic Transmission Through Fuselage Panel-Frame Structures," 118th Meeting of the Acoustical Society of America, St. Louis, Missouri, November, 1989.

D. B. Bliss and J. A. Gottwald, "Low Frequency Transmission Loss by Alternate Resonance Tuning (ART)," 117th Meeting of the Acoustical Society of America, Syracuse, New York, May, 1989 (presented by J. A. Gottwald).

D. B. Bliss and J. A. Gottwald, "Reduction of Sound Transmission Through Fuselage Walls by Alternate Resonance Tuning (ART)," 12th Aeroacoustics Conference, San Antonio, Texas, April, 1989 (presented by D. B. Bliss).

D. B. Bliss, "Analysis of Acoustic Transmission Through Fuselage Panel-Frame Structures,"12th Aeroacoustics Conference, San Antonio, Texas, April, 1989 (presented by D. B. Bliss).

SECTION 2.2 PAPERS TO DATE

D. B. Bliss and J. A. Gottwald, "Reduction of Sound Transmission Through Fuselage Walls by Alternate Resonance Tuning (ART)," accepted for publication by the AIAA Journal of Aircraft, and currently in revision.

D. B. Bliss, J. A. Gottwald, and M.B. Gustaveson, "Alternate Resonance Tuning With Non-Uniform Incident Pressure Field Considerations, Including a Comparison With Experiment," in preparation.

D. B. Bliss, "Analysis of Sound Transmission Through Flexible Panel/Frame Walls," in preparation, copy attached.

D. B. Bliss and R. Srinivasan, "High Frequency Alternate Resonance Tuning", in preparation, copy attached.

J. A. Gottwald and D. B. Bliss, "Alternate Resonance Tuning With Real Panel Considerations," in preparation.

SECTION 2.3 DISSERTATIONS

J. A. Gottwald, "Noise Reduction for Panelled Structures Using Alternate Resonance Tuning", Doctoral Dissertation in preparation, Duke University, Department of Mechanical Engineering and Materials Science, Fall, 1990.

Srinivasan, R, "A Study of Alternate Resonance Tuning Configurations", Masters Dissertation, Duke University, Department of Mechanical Engineering and Materials Science, June, 1990.

SECTION 3. THEORETICAL ANALYSIS

Model problem development and analysis continues with the Alternate Resonance Tuning concept. This section highlights the current ongoing analytic tasks. The various topics described below are presently at different stages of completion. These topics include the following:

- investigation of the ART effect with real panel sections;

- investigation of the effectiveness of the ART concept under an external propagating pressure field simulating propeller passage effects on the fuselage;

- development of a new method of analysis which has broad application to panel/frame structures at relatively low frequencies and also provides a general analytical formulation for noise reduction concepts involving structural tuning;

- parametric studies using existing ART computer programs to further explore the method's usefulness;

- model problems involving the ART concept for high frequency noise reduction.

- analysis of ART performance with a double panel wall using a new panel analysis method;

- numerical investigation linking existing experimental data with existing theory through variation of system parameters via least squares data fitting.

Section 3a: Modelling the ART Concept Using Real Panel Sections

The analysis of the ART concept using real panel sections has been completed, and appropriate computer models are now in the development stage. This problem deals with the performance of ART-tuned real plate sections in an appropriate ART 4-panel analysis configuration. The most general analytic configuration is shown in Figure 3a-1. This geometry simply includes a standard four panel array, two panels on top and two panels on the bottom. Four panels for

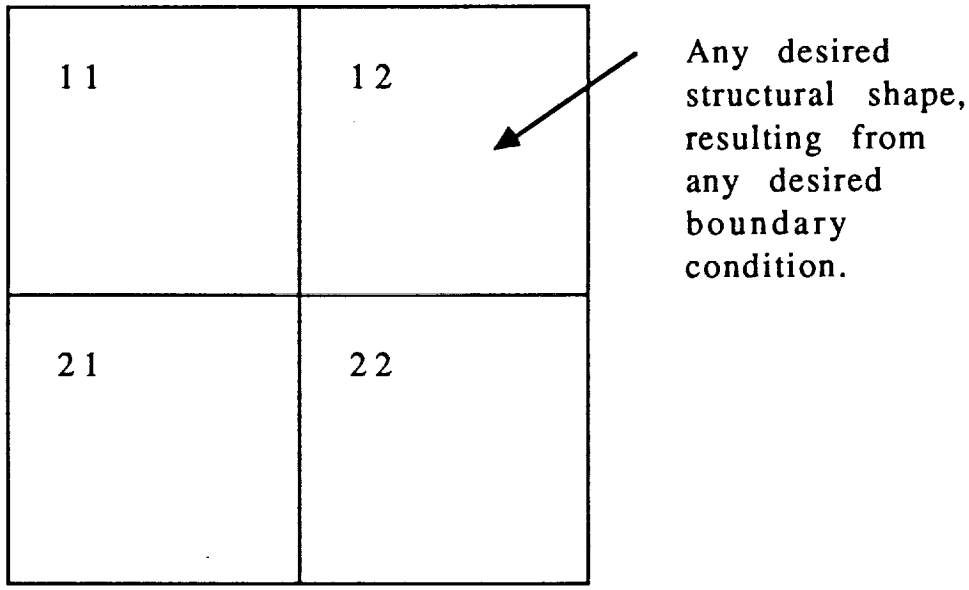

Figure 3a-1: Configuration for ART Real Panel Analysis

each identical panel subsystem have been chosen as a convenient number for equation derivation, but in reality, any rectangular array of panels may be considered. For the present case, panels are numbered in the standard matrix-like notation as shown. Note that no restriction has been placed on the boundary conditions of each panel. The latter assumption allows the analysis to proceed most generally, and at a later appropriate

time, the boundary conditions will be chosen through specification of the appropriate structural mode shapes for the panels. The panel array is considered to be one subsystem mounted on an infinite wall composed of infinitely many panel subsystems. An anechoic termination is assumed beyond the wall.

To formulate the governing equations, consider panel 11 (an arbitrary choice). A general acoustic velocity function may be defined as

$$u(x,y,z,t) = \sum_i \sum_j U_{ij}\, \psi_{ij}(y,z)\; e^{i(\omega t - k_{x_{ij}} x)} \qquad (3a\text{-}1)$$

where the subscript indices i and j refer to acoustic modes, and $\psi_{ij}(y,z)$ describes the spatial dependence of an acoustic modal function. U_{ij} is the corresponding complex acoustic modal velocity amplitude. Note that the acoustic modes are harmonic in time and propagating in the +x direction. Similarly, a general acoustic pressure may be expressed as

$$p(x,y,z,t) = \sum_i \sum_j P_{ij}\, \psi_{ij}(y,z)\; e^{i(\omega t - k_{x_{ij}} x)} \qquad (3a\text{-}2)$$

with P_{ij} representing the complex pressure amplitude of acoustic mode ij. Note that the relationship

$$P_{ij} = \rho_o \frac{\omega}{k_{x_{ij}}} U_{ij} \qquad (3a\text{-}3)$$

may be defined as a consequence of the x-component of the momentum equation.

For the structural problem, the wall displacement may be denoted as

$$\xi_w(y,z,t) = \sum_p \sum_q A_{pq}^{11} \phi_{pq}^{11}(y,z)\ e^{i\omega t} \qquad (3a\text{-}4)$$

where A_{pq}^{11} is the complex structural modal amplitude for mode pq of panel 11 and ϕ_{pq}^{11} is the individual panel shape function for mode pq of panel 11. A convention is made here that superscripts will always refer to the plate location as per Figure 3a-1; subscripts will always refer to either acoustic modes using i and j, or structural modes using p and q. Note that the overall wall shape function ψ and the individual panel shape function ϕ are separable functions; that is, for panel 11,

$$\phi_{pq}^{11}(y,z) = \Phi_p(y)\ \Phi_q(z)$$

$$\psi_{pq}^{11}(y,z) = \Psi_p(y)\ \Psi_q(z)$$

Differentiation of Equation (3a-4) results in an expression for the wall velocity as

$$u_w = \frac{\partial \xi_w}{\partial t}(y,z,t) = \sum_p \sum_q i\omega A_{pq}^{11} \phi_{pq}^{11}(y,z)\ e^{i\omega t} \qquad (3a\text{-}5)$$

The acoustic and structural equations are linked at the panel/fluid interface, or at x = 0, where the acoustic velocity is equivalent to the wall velocity

$$u_{acoustic}(0,y,z,t) = u_{wall}(0,y,z,t) \qquad (3a\text{-}6)$$

This boundary condition encourages placement of Equation 3a-1 equal to Equation 3a-5 at x = 0, resulting in

$$\sum_i \sum_j U_{ij}\, \psi_{ij}(y,z) = \sum_p \sum_q i\omega A_{pq}^{11}\, \phi_{pq}^{11}(y,z) \qquad (3a\text{-}7)$$

The acoustic modes and the structural modes each form an orthogonal set with respect to themselves. However, the acoustic modes are not necessarily orthogonal to the structural modes. Application of orthogonality to Equation 3a-7, and substituting dS = dydx yields

$$\sum_i \sum_j U_{ij} \int_{S_{total}} \psi_{ij}\, \psi_{ij} dS_{total} = \sum_p \sum_q i\omega A_{pq}^{11} \int_{S_{11}} \psi_{rs}\, \phi_{pq}^{11} dS_{11} \qquad (3a\text{-}8)$$

The only modes of the left hand side of Equation 3a-8 which survive are Ψ_{rs}. Therefore, with a change in indices,

$$U_{ij}^{11} = \frac{\sum_p \sum_q i\omega A_{pq}^{11} \int_{S_{11}} \psi_{ij}\, \phi_{pq}^{11}\, dS_{11}}{\int_{S_{total}} \psi_{ij}^2\, dS_{total}} \qquad (3a\text{-}9)$$

By virtue of the momentum equation invoked to produce Equation 3a-3, the complex acoustic pressure amplitudes may be expressed as

$$P_{ij}^{11} = \frac{\sum_p \sum_q i\rho\omega^2 \int_{S_{11}} \psi_{ij}\, \phi_{pq}^{11}\, dS_{11}}{k_{x_{ij}} \int_{S_{total}} \psi_{ij}^2\, dS_{total}} A_{pq}^{11} \qquad (3a\text{-}10)$$

A convenient notational shorthand allows the expression of Equation 3a-10 in a more compact form

$$P_{ij}^{11} = \sum_{p} \sum_{q} T_{ijpq}^{11} A_{pq}^{11} \qquad (3a\text{-}11)$$

where

$$T_{ijpq}^{11} = \left[\frac{i\rho\omega^2 \int_{S11} \psi_{ij} \phi_{pq}^{11} \, dS_{11}}{k_{xij} \int_{S_{total}} \psi_{ij}^2 \, dS_{total}} \right] \qquad (3a\text{-}12)$$

Note an additional notational convention where $S_p{}^{11}$ is the area of the single panel 11; its associated derivative $dS_p{}^{11}$ in integral equations implies integration over the surface of panel 11. Similarly, S_{total} is the area of the entire panel array (equal to 4 times the panel width W times the panel height H); the associated derivative dS_{total} in integral equations implies integration over the entire panel assembly.

Lagrange's equations may be used to derive the equations of motion for the panel structure itself.* In general

$$M_{pq}^{11} \left[\left(A_{pq}^{11} e^{i\omega t} \right)_{tt} + 2\zeta_{pq}^{11} \omega_{npq}^{11} \left(A_{pq}^{11} e^{i\omega t} \right)_{t} \right] + \omega_{npq}^{11\,2} \left(A_{pq}^{11} e^{i\omega t} \right) = Q_{pq}^{11} e^{i\omega t} \qquad (3a\text{-}13)$$

where $M_{pq}{}^{11}$ is the generalized mass of mode pq of panel 11, $\zeta_{pq}{}^{11}$ is the damping ratio of mode pq of panel 11, $\omega_{npq}{}^{11}$ is the undamped natural frequency of mode pq of panel 11, and $Q_{pq}{}^{11}$ is the sum total of all generalized forces acting on panel 11.

In particular, the generalized forces are worth further perusal. The right hand side of Equation 3a-13 (without the

* See, for example, Dowell, E.H., et. al., *A Modern Course in Aeroelasticity*, Sijthoff and Noordhoff International Publishers, Alphen aan den Rijn, The Netherlands, 1978.

harmonic excitation $e^{i\omega t}$) may be expressed in general for any panel $\alpha\beta$ as

$$Q_{pq}^{\alpha\beta} = \sum_a \sum_b Q_{m_{pq}}^{\alpha\beta,ab} + Q_E^{\alpha\beta} \qquad (3a\text{-}14)$$

where the term Q_E is the external forcing term, resulting from holding the wall fixed and observing the incident wave exhibit a hard wall reflection on panel $\alpha\beta$. The summation term is a convenient way of representing the generalized force contribution of all panels in the entire panelled system on panel $\alpha\beta$ where the analysis is focused. The notation represents the effect of the motion of mode pq of panel ab on panel $\alpha\beta$. In more general form, Equation 3a-14 may be written for the four panel analysis configuration focusing on panel $\alpha\beta$ as

$$Q_{pq}^{\alpha\beta} = \sum_a \sum_b Q_{m_{pq}}^{\alpha\beta,ab} + Q_E^{\alpha\beta} = Q_{m_{pq}}^{\alpha\beta,11} + Q_{m_{pq}}^{\alpha\beta,12} + Q_{m_{pq}}^{\alpha\beta,21} + Q_{m_{pq}}^{\alpha\beta,22} + Q_E^{\alpha\beta} \qquad (3a\text{-}15)$$

Here the subscript m indicates a generalized force resulting from motion of panel ab on $\alpha\beta$. Equations 3a-14 and 3a-15 are a direct result of the concept of superposition applied to the panel subject to analysis.

Note that the generalized force on the right hand side of Equation 3a-15 may be written as

$$Q_{m_{pq}}^{\alpha\beta,ab} = \int \phi_{pq}^{\alpha\beta}\, p^{ab}\,(0,y,z)\, dS_p^{\alpha\beta} \qquad (3a\text{-}16)$$

$p^{ab}(0,y,z)$ may be replaced using Equation (3a-2) as

$$p^{ab}(0,y,z) = \sum_i \sum_j P_{ij}^{ab} \psi_{ij}(y,z) dS_p^{ab} \qquad (3a\text{-}17)$$

Substitution of Equation 3a-11 for P_{ij}^{ab} and back substitution of Equation 3a-17 into 3a-16 yields the generalized force on panel $\alpha\beta$ as a result of the motion of panel ab as

$$Q_{m_{pq}}^{\alpha\beta,ab} = \int \phi_{pq}^{\alpha\beta}(y,z) \sum_i \sum_j \sum_c \sum_d T_{ijcd}^{ab} A_{cd}^{ab} \psi_{ij}(y,z) \, dS_p^{\alpha\beta} \qquad (3a\text{-}18)$$

Furthermore, substitution into 3a-18 yields

$$\int \phi_{pq}^{\alpha\beta} \sum_i \sum_j \psi_{ij} \, dS_p^{\alpha\beta} = \frac{k_{x_{ij}}}{i\rho_0\omega^2} \int \psi_{ij}^2 \, dS_{Total} * T_{ijpq}^{\alpha\beta} \qquad (3a\text{-}19)$$

where a panel independent quantity J_{ij} may be written as

$$J_{ij} = \frac{k_{x_{ij}}}{i\rho_0\omega^2} \int \psi_{ij}^2 \, dS_{total} \qquad (3a\text{-}20)$$

Therefore, the entire generalized force on $\alpha\beta$ will consist of one contribution from each panel, and may be most compactly represented as

$$\sum_a \sum_b Q_{m_{pq}}^{\alpha\beta,ab} + Q_{E_{pq}}^{\alpha\beta} = \sum_a \sum_b \left[\sum_c \sum_d A_{cd}^{ab} \sum_i \sum_j J_{ij} \, T_{ijpq}^{\alpha\beta} T_{ijcd}^{ab} + Q_{E_{pq}}^{\alpha\beta} \right] \qquad (3a\text{-}21)$$

With the help of Equation 3a-13 expressed in the most general form for any panel, the panel governing equations may be written as a linear system of the form

$$\sum_{\alpha}\sum_{\beta}\sum_{p}\sum_{q}\left[A_{pq}^{\alpha\beta} M_{pq}^{\alpha\beta} + \sum_{a}\sum_{b}\left[\sum_{c}\sum_{d} A_{cd}^{ab} \sum_{i}\sum_{j} J_{ij}\, T_{ijpq}^{\alpha\beta} T_{ijcd}^{ab}\right]\right] = Q_{E_{pq}}^{\alpha\beta} \tag{3a-22}$$

where $M^{\alpha\beta}_{pq}$ is the result of using Lagrange's equations to represent the panel dynamics,

$$M_{pq}^{\alpha\beta} = M_{pq}^{\alpha\beta}\left[\left(A_{pq}^{\alpha\beta} e^{i\omega t}\right)_{tt} + 2\zeta_{pq}^{\alpha\beta}\,\omega_{n_{pq}}^{\alpha\beta}\left(A_{pq}^{\alpha\beta} e^{i\omega t}\right)_{t} + \omega_{n_{pq}}^{\alpha\beta^2}\left(A_{pq}^{\alpha\beta} e^{i\omega t}\right)\right] \tag{3a-23}$$

$QE^{ab}{}_{pq}$ is the external forcing, and the complex modal panel amplitudes $A^{\alpha\beta}{}_{pq}$ are the solutions to the linear system.

Expression of Equation (3a-22) in nondimensional terms allows for the most general engineering interpretations. Note that in the combination of J_{ij}, $T^{\alpha\beta}{}_{ijpq}$, and $T^{ab}{}_{ijcd}$, some simplification occurs; also, the external generalized force is now stated explicitly in nondimensional terms, resulting in

$$\sum_{\alpha=1}^{yp}\sum_{\beta=1}^{zp}\sum_{p=1}^{sm}\sum_{q=1}^{sm}\left[\bar{\nu}_{\alpha\beta pq} + \sum_{a=1}^{yp}\sum_{b=1}^{zp}\sum_{c=1}^{sm}\sum_{d=1}^{sm}\bar{\eta}_{abcd\alpha\beta pq} = \bar{\kappa}_{\alpha\beta pq}\right] \tag{3a-24}$$

where the nondimensional terms ν, η, and κ are denoted by

$$\nu_{\alpha\beta pq} = \left(\frac{S_1}{S_2}\right)\bar{A}_{pq}^{\alpha\beta}\,\bar{M}_{pq}^{\alpha\beta}\left[\,\bar{\omega}_{n_{pq}}^{\alpha\beta^2} + 2i\,\zeta_{pq}^{\alpha\beta}\,\bar{\omega}\,\bar{\omega}_{n_{pq}}^{\alpha\beta} - \bar{\omega}^{\,2}\,\right] \tag{3a-25}$$

$$\bar{\eta}_{abcd\alpha\beta pq} = i\bar{\omega}^2 \bar{A}_{cd}^{ab} \sum_{i=0}^{am} \sum_{j=0}^{am} \bar{\phi}_{pq}^{\alpha\beta} \psi_{ij} \, dS_p^{\alpha\beta} \left(\frac{\omega_r}{k_{x_{ij}}}\right) \frac{\int \bar{\phi}_{pq}^{ab} \psi_{ij} \, dS_p^{ab}}{\int \psi_{ij}^2 \, dS_{total}} \tag{3a-26}$$

$$\bar{\kappa}_{\alpha\beta pq} = \int \bar{\phi}_{pq}^{\alpha\beta} dS_p^{\alpha\beta} \tag{3a-27}$$

Additionally, from Equation (3a-24), yp is the number of panels in the model in the y direction (assumed to be equal to 2), zp is the number of panels in the
z direction (assumed to be 2), and sm is the number of structural modes to be included in the calculation. From Equation (3a-25), other nondimensional variables include

$$S_1 = \frac{\omega_r H}{c}$$

$$S_2 = \frac{\rho \, W \, H^2}{m_{11}}$$

where ω_r is a user-chosen reference frequency, usually set to the lowest ART cancellation frequency, H is the panel height, c is the speed of sound in air,
ρ is the density of air surrounding the panels, W is panel width, and m_{11} is the mass of panel 11 as shown in Figure 3a-1;

$$\bar{A}_{pq}^{\alpha\beta} \equiv \frac{\omega_r \, A_{pq}^{\alpha\beta} \, \rho \, c}{P_E}$$

is the complex nondimensional modal amplitude for mode pq of panel $\alpha\beta$, where P_E is the total external pressure on panel ab equal to $(2P_i - P_t)$. P_i is the incident pressure on the upstream

panel side, and P_t is the transmitted pressure through the panel array. Other nondimensional relationships from Equation (3a-25) are defined as follows:

$$\overline{M}_{pq}^{\alpha\beta} = \frac{m_{pq}^{\alpha\beta}}{m_{11}^{11}}$$

$$\overline{\omega}_{n_{pq}}^{\alpha\beta} \equiv \frac{\omega_{n_{pq}}^{\alpha\beta}}{\omega_r}$$

$$\overline{\omega} \equiv \frac{\omega}{\omega_r}$$

From Equation (3a-26), note that am is the number of acoustic modes considered in the system. The nondimensional panel shape function is defined as

$$\overline{\phi}_{pq}^{\alpha\beta} \equiv \phi(\overline{y},\overline{z}) \equiv \phi\left(\frac{y}{W}, \frac{z}{H}\right)$$

Note that the quantity

$$\left(\frac{\omega_r}{k_{xij}}\right)$$

is nondimensional; however, the actual form of k_{xij} cannot be determined until an appropriate choice for ψ_{ij} has been determined; ω_r will then be used to nondimensionalize the frequency appearing in the k_{xij}.

Recovering Some Familiar Results From the General Real Panel Analysis

A number of familiar example problems may be recovered from the real panel governing equations, either in dimensional form, such as Equation 3a-22 (with appropriate substitution for

the elements $M^{\alpha\beta}{}_{pq}$, J_{ij}, $T^{\alpha\beta}{}_{ijpq}$, $QE^{\alpha\beta}{}_{pq}$, and $T^{ab}{}_{ijcd}$), or in nondimensional form, such as Equations 3a-24 through 3a-27.

The most basic example which can be recovered is the case of a single panel in an infinite duct. After appropriate substitution, Equation 3a-22, the general dimensional governing equation, reduces to (neglecting all summation limits temporarily)

$$\sum_{\alpha}\sum_{\beta}\sum_{p}\sum_{q} A_{pq}^{\alpha\beta} M_{pq}^{\alpha\beta}\left[\omega_{n_{pq}}^{\alpha\beta\,2} + 2i\,\zeta_{pq}^{\alpha\beta}\,\omega\,\omega_{n_{pq}}^{\alpha\beta} - \omega^{2}\right]$$

$$- \sum_{c}\sum_{d}\sum_{r}\sum_{s} A_{rs}^{cd} \sum_{i}\sum_{j} \int \phi_{pq}^{\alpha\beta}\,\psi_{ij}\,dS_{p}^{\alpha\beta}\left(\frac{i\rho\omega^{2}}{k_{x_{ij}}}\right)\frac{\int \phi_{pq}^{cd}\,\psi_{ij}\,dS_{p}^{cd}}{\int \psi_{ij}^{2}\,dS_{total}} = P_{E}\int \phi_{pq}^{\alpha\beta}\,dS_{p}^{\alpha\beta} \qquad (3a\text{-}28)$$

For a single panel in a duct, all acoustic modes except the one dimensional mode may be ignored; as such, $\psi_{ij} \rightarrow 1$ and $k_{xij} \rightarrow \omega/c$. For a flat panel, the mode shape $\phi \rightarrow 1$; all summations can be removed. From Equation 3a-28, the ratio of the integral over $dS_p{}^{cd}$ to the integral over $dS_{total} \rightarrow 1.0$ Equation 3a-28 reduces to

$$A\,M\left[\omega_{n}^{2} + 2i\zeta\omega\omega_{n} - \omega^{2}\right] - iAWH\rho\omega c = P_{E}WH \qquad (3a\text{-}29)$$

Note that $i\omega A = U$, the panel velocity; also, $p_t = \rho c U$. M, the mass per unit area, may be replaced by m, the panel mass. From a fixed wall approximation, $P_E = 2P_I$. These manipulations yield

$$\frac{U}{WH}\,m\frac{\left[\omega_{n}^{2} + 2i\zeta\omega\omega_{n} - \omega^{2}\right]}{i\omega} - P_{t} = 2P_{I} \qquad (3a\text{-}30)$$

The panel's mechanical impedance may be expressed in the familiar form

$$Z_m = R + i\left[m\omega - \frac{s}{\omega}\right] \qquad (3a\text{-}31)$$

where R is the mechanical damping and s is the spring constant. Also,

$$\zeta = \frac{R\omega_n}{2s} \qquad (3a\text{-}32)$$

Substitution of 3a-31 and 3a-32 into 3a-30 yields a familiar relationship for the ratio of transmitted to incident pressure in a duct as

$$\frac{P_t}{P_I} = \frac{2}{\frac{Z_m}{WH\rho c} - 1} \qquad (3a\text{-}33)$$

A second limit that can be recovered is the branch analysis relationship for the ART 4-panel geometry in a duct.* The branch analysis result gives the ratio of the transmitted pressure to the incident pressure across the panel barrier in a duct when only the one dimensional acoustic mode is considered. In dimensional form for an anechoic termination,

$$\frac{P_T}{P_I} = \frac{\Delta}{\Delta + \frac{2}{\rho cWH} Z_{11}\ Z_{12}\ Z_{21}\ Z_{22}} \qquad (3a\text{-}34)$$

where

$$\Delta = Z_{11}\,Z_{12}\,Z_{21} + Z_{11}\,Z_{12}\,Z_{22} + Z_{11}\,Z_{21}\,Z_{22} + Z_{12}\,Z_{21}\,Z_{22}$$

Note that all impedances in Equation 3a-34 are mechanical impedances, of the form as shown in Equation 3a-31. Again, $\psi_{ij} \rightarrow 1$, $k_{xij} \rightarrow \omega/c$, and the panel mode shape $\phi \rightarrow 1$. With respect to the dimensional governing Equation 3a-28, summation over the

* D. B. Bliss and J. A. Gottwald, "Reduction of Sound Transmission Through Fuselage Walls by Alternate Resonance Tuning (ART)", accepted for publication in the AIAA *Journal of Aircraft*, in final revision.

panel indices $\alpha\beta$ and cd from 1 to 2 is now required. Following a similar logic as that described to derive the governing equation for a single panel in a duct, Equation 3a-28 will reduce to a system of four nondimensional equations of the form

$$\bar{U}_{11}\left[\left(\frac{S_1}{S_2}\right)\bar{Z}_{m11}+\frac{1}{4}\right]+\frac{\bar{U}_{12}}{4}+\frac{\bar{U}_{21}}{4}+\frac{\bar{U}_{22}}{4}+\bar{P}_T=2$$

$$\frac{\bar{U}_{11}}{4}+\bar{U}_{12}\left[\left(\frac{S_1}{S_2}\right)\bar{Z}_{m12}+\frac{1}{4}\right]+\frac{\bar{U}_{21}}{4}+\frac{\bar{U}_{22}}{4}+\bar{P}_T=2$$

$$\frac{\bar{U}_{11}}{4}+\frac{\bar{U}_{12}}{4}+\bar{U}_{21}\left[\left(\frac{S_1}{S_2}\right)\bar{Z}_{m21}+\frac{1}{4}\right]+\frac{\bar{U}_{22}}{4}+\bar{P}_T=2$$

$$\frac{\bar{U}_{11}}{4}+\frac{\bar{U}_{12}}{4}+\frac{\bar{U}_{21}}{4}+\bar{U}_{22}\left[\left(\frac{S_1}{S_2}\right)\bar{Z}_{m22}+\frac{1}{4}\right]+\bar{P}_T=2$$

(3a-35(a-d))

where nondimensional velocities are denoted by

$$\bar{U}_{ij}=\frac{U_{ij}\,\rho\,c}{P_I}$$

and nondimensional impedances are given by

$$\bar{Z}_{mij}=\overline{MR}_{ij}\,\bar{\omega}_{ij}\left[2\zeta_{ij}+i\left(\frac{\bar{\omega}}{\bar{\omega}_{ij}}-\frac{\bar{\omega}_{ij}}{\bar{\omega}}\right)\right]$$

Additionally, mass ratios are defined as

$$\overline{MR}_{ij}\equiv\frac{m_{ij}}{m_{11}}$$

and

$$\overline{P}_T \equiv \frac{P_T}{P_I}$$

Other relationships have been defined previously. Finally, a fifth equation expresses the fact that the resultant nondimensionalized pressure ratio is an average of all nondimensional panel velocities; that is,

$$\frac{\overline{U}_{11}}{4} + \frac{\overline{U}_{12}}{4} + \frac{\overline{U}_{21}}{4} + \frac{\overline{U}_{22}}{4} - \overline{P}_T = 0 \qquad \text{(3a-35e)}$$

With the aid of the symbolic manipulation program *Mathematica*, Equations 3a-35 can be solved for the unknowns U_{11}, U_{12}, U_{21}, U_{22}, and P_T. In nondimensional form, P_T is the equivalent of the dimensional branch analysis relationship shown in 3a-34

$$\overline{P}_T = \frac{\overline{\Delta}}{\overline{\Delta} + \left(\frac{S_1}{S_2}\right) \overline{Z}_{11}\ \overline{Z}_{12}\ \overline{Z}_{21}\ \overline{Z}_{22}} \qquad \text{(3a-36)}$$

where

$$\overline{\Delta} = \overline{Z}_{11}\,\overline{Z}_{12}\,\overline{Z}_{21} + \overline{Z}_{11}\,\overline{Z}_{12}\,\overline{Z}_{22} + \overline{Z}_{11}\,\overline{Z}_{21}\,\overline{Z}_{22} + \overline{Z}_{12}\,\overline{Z}_{21}\,\overline{Z}_{22}$$

Research effort will now focus on the computational code to solve Equation 3a-24. A structural branch analysis computational code is currently in development. As with the simple branch analysis results shown in Equations 3a-34 and 3a-36, the structural branch analysis system will be of the order (number of structural modes times number of panels). This code also considers ψ_{ij} to equal one in order to simplify the programming.

Section 3b: External Pressure Field Modeling

The purpose of this investigation is to determine the effectiveness of the ART concept under an external propagating pressure field such as that which might be associated with propeller passage by an aircraft fuselage. In general, the problem deals with modeling the interaction of fluid and structural components within the realm of ART tuning. The derivation of the system governing equations was presented in the December, 1989 progress report. For convenience, the analysis schematic for the system is reproduced in Figure 3b-1. Additional recent results of interest follow, produced from parametric studies using all existing computer codes.

For the geometry shown in Figure 3b-1, the mode turn-on frequencies are shown in Figure 3b-2. It has been determined that locating the ART frequency (that is, the frequency of greatest noise reduction) near a mode turn-on frequency will destroy some, if not all, of the ART cancellation effect. (Note that in Figure 3b-2, the zero mode, commonly called the "1-D mode," always propagates.) Therefore, for the runs shown in this section, the ART design frequency was placed at nondimensional frequency $\omega = 1.5$ by placing panel resonances at $\omega = 0.8$ and $\omega = 2.0$.

In the following technical discussion, note that the data shown in Figures 3b-3 through 3b-6 were generated using 16 panels in the sweep model geometry. 64 acoustic modes were carried for the solution. Noise reduction across the ART barrier is plotted in dB against nondimensional frequency. In these plots, the location of the noise reduction calculation point was 64 individual panel lengths (4 overall duct heights) downstream, and at a point just under the top of the duct, at $z = 0.96875$.

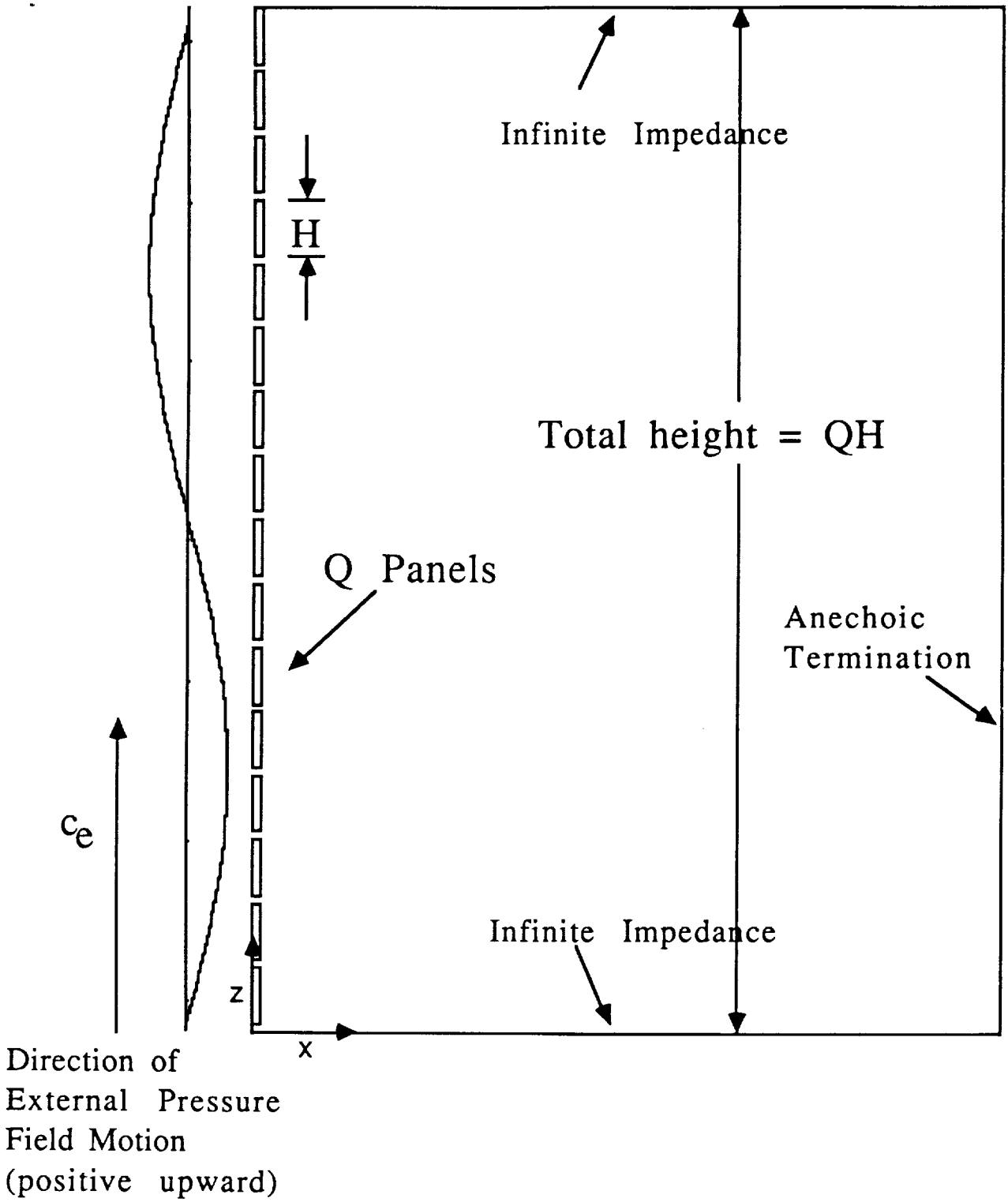

Figure 3b-1: Velocity Sweep Analysis Configuration

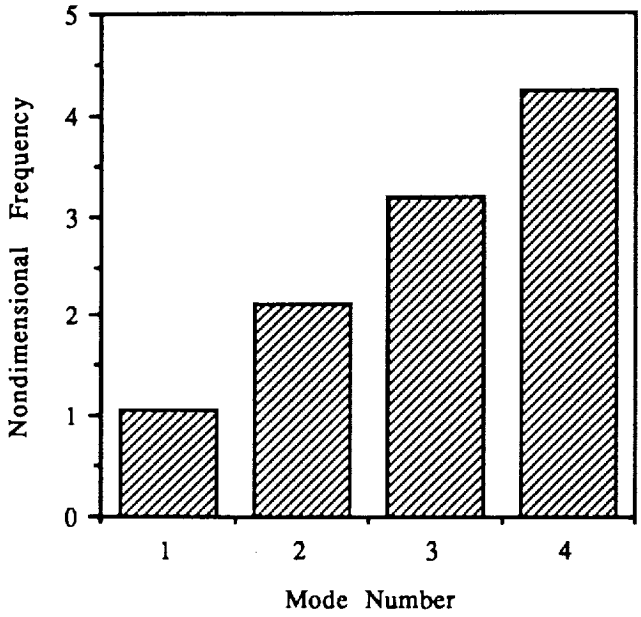

Figure 3b-2: Mode turn-on frequencies for the geometry shown in Figure 3b-1.

Figure 3b-3 shows the noise reduction calculation for both ART and identical panels when there is no sweep velocity present on the panel barrier exterior. The ART calculation looks much like the calculation performed with the basic 2 or 4 panel theory, except there is a small effect at some mode turn-on points. The identical calculation forces all panels to behave in a similar manner; this result is equivalent to the branch analysis result (where apparent mass effects have no bearing on the noise reduction result). In this case, obviously the ART-tuned panels are a clear winner.

Figure 3b-4 Shows a similar calculation, except here the sweep speed is 20% above Mach 1. As mentioned earlier, the ART nondimensional design frequency for these cases was set at $\omega = 1.5$. Due to the sweeping effect, this

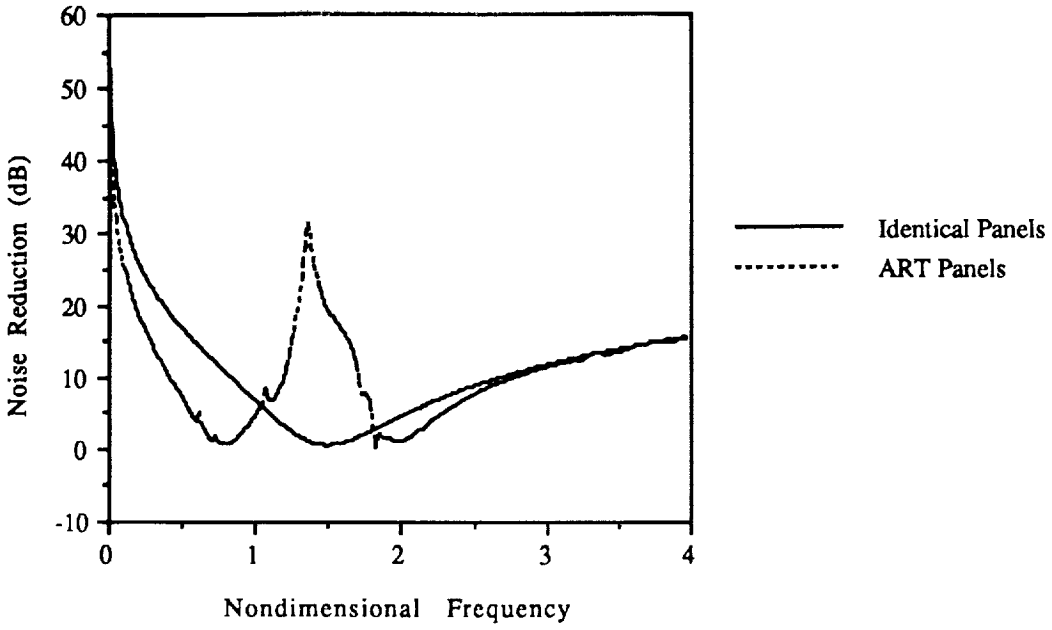

Figure 3b-3: Noise reduction for identical and ART panels in the sweep geometry; 16 panels, no sweep.

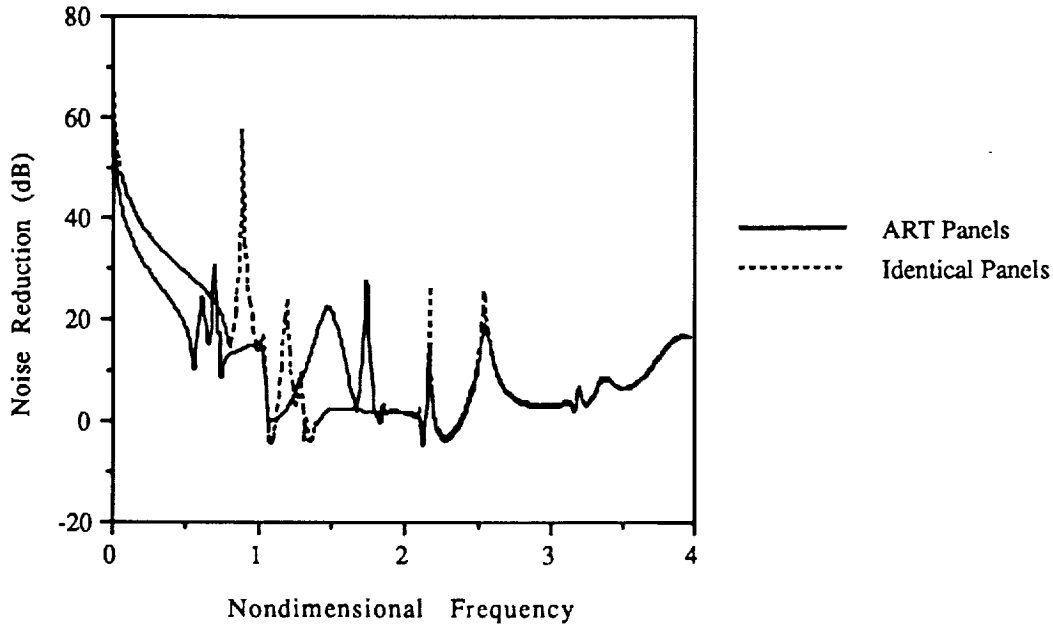

Figure 3b-4: Noise reduction in dB for identical and ART panels for the sweep geometry. External sweep speed is 20% above Mach 1.

frequency is lowered by a small amount to $\omega = 1.48$. At the ART design frequency, there is a noise reduction of over 20 dB. Note the dramatic effects due to mode turn-on, an unavoidable occurrence. Higher frequencies show almost identical noise reduction results for identical and ART tuned panels.

In Figure 3b-5, the sweep speed is reduced to Mach 1. Again the ART panels show a noise reduction of about 20 dB at $\omega = 1.48$. Similarly, Figure 3b-6 shows a noise reduction of just under 20 dB for a sweep speed at 20% below Mach 1.

Another interesting (and perhaps less traditional) method to compare the ART panel tuning against the identical panel tuning is to look at the modal contributions from the coefficients of the pressure expansion. Figures 3b-7 through 3b-9 show the negative of the log of the coefficients calculated for the pressure expansion in the duct for both ART and identical panels. These values were calculated much closer to the panel barrier than the results in Figures 3b-3 through 3b-6; the calculation was performed at a point 8 individual panel lengths (or half the duct height) downstream of the panel barrier. On the x axis, mode 0 is listed as 1, mode 1 is listed as 2, and so forth. Figure 3b-7 shows values for a sweep speed of 20% above Mach 1; Figure 3b-8 shows values for a sweep speed of Mach 1, and Figure 3b-9 shows values for a sweep speed of 20% less than Mach 1. In all cases, the ART tuned panels are showing a greater contribution to the overall noise reduction in every mode of the pressure expansion, and at all ranges of sweep speed tested.

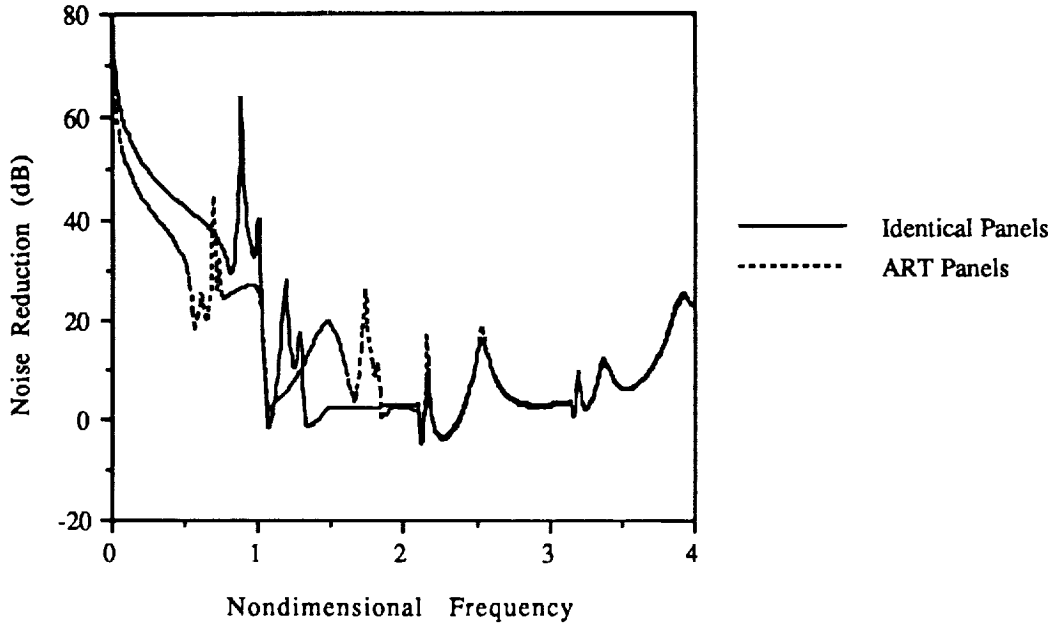

Figure 3b-5: Noise reduction across identical and ART panels in the sweep problem with sweep speed at Mach 1.

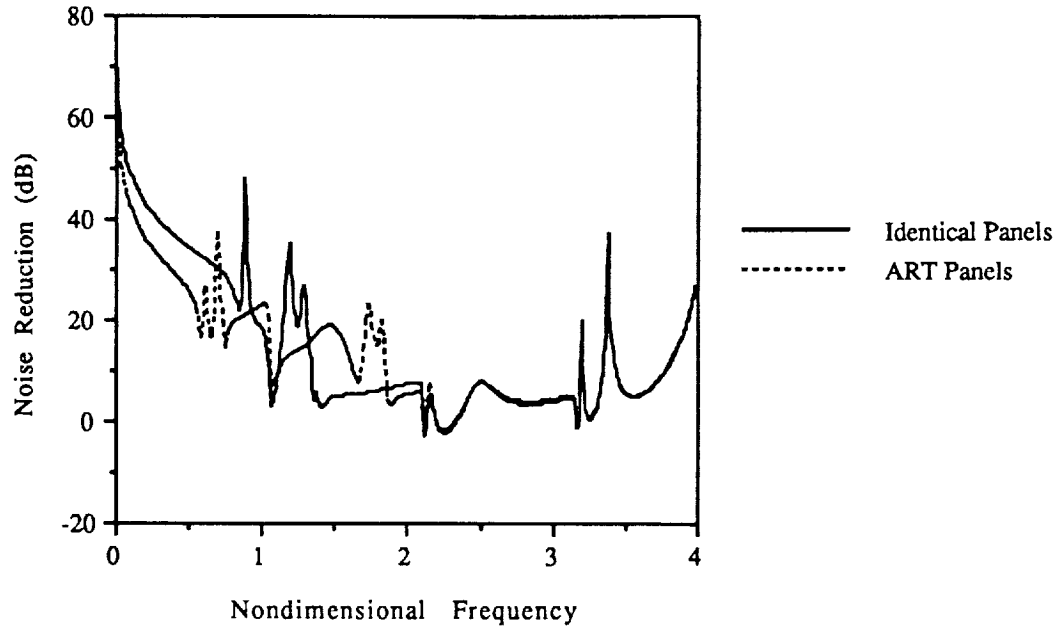

Figure 3b-6: Noise reduction across identical and ART panels in the sweep problem with sweep speed at 20% below Mach 1.

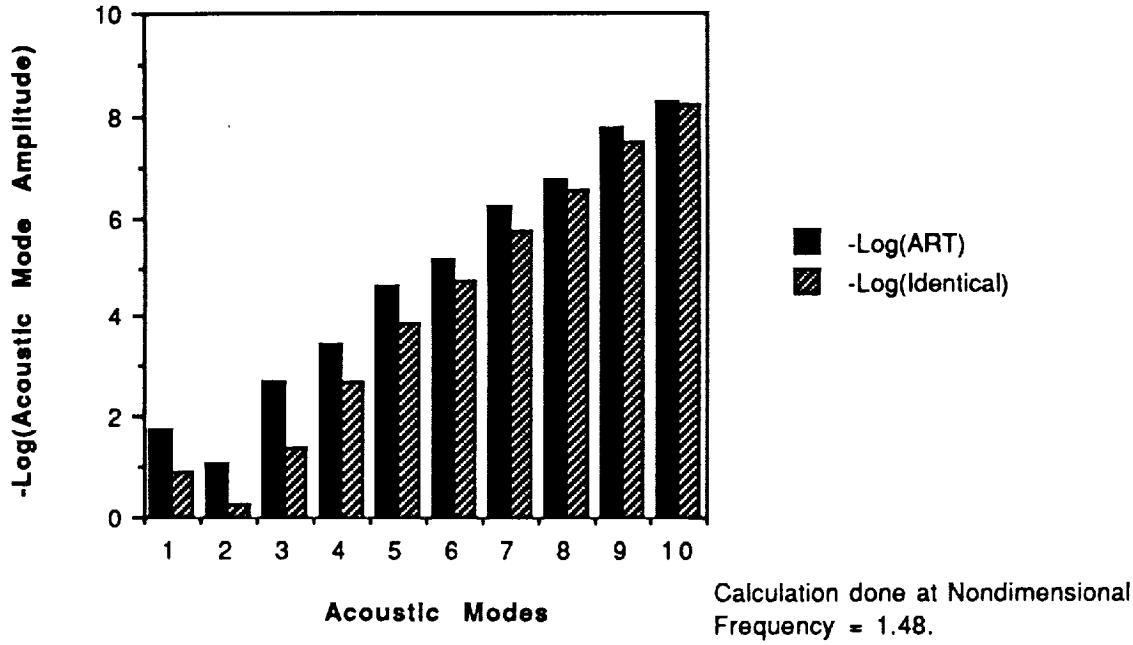

Figure 3b-7: Relative comparison of first 10 modal contributions to noise reduction in the sweeping problem. Sweep speed is 20% above Mach 1. See text for details.

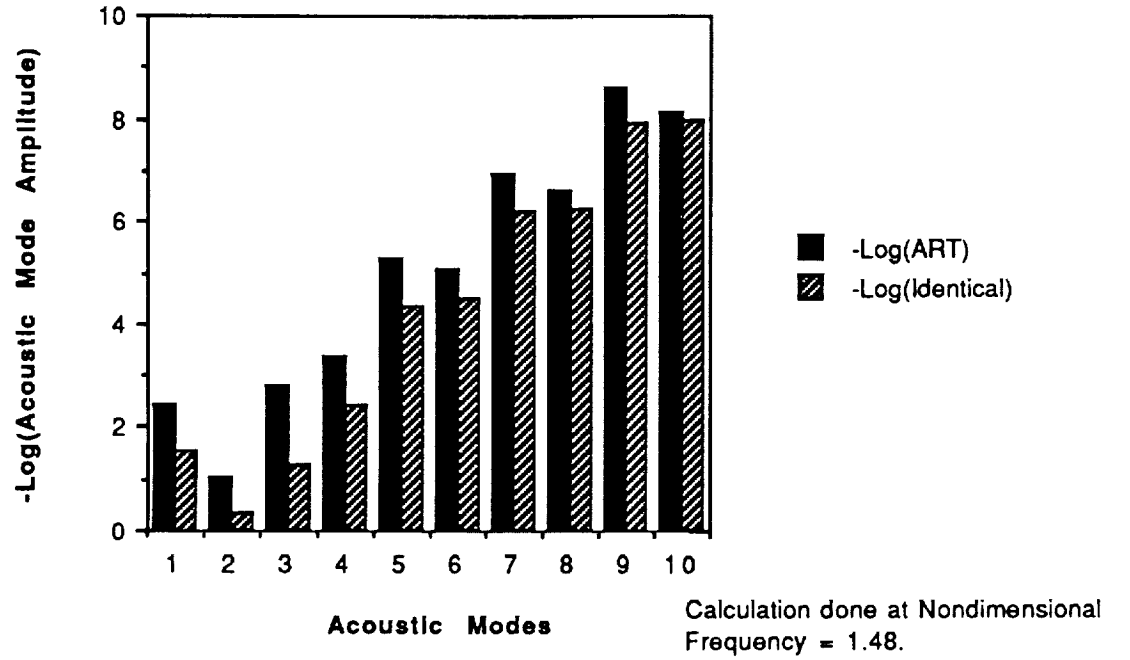

Figure 3b-8: Relative comparison of first 10 modal contributions to noise reduction in the sweeping problem. Sweep speed is at Mach 1. See text for details.

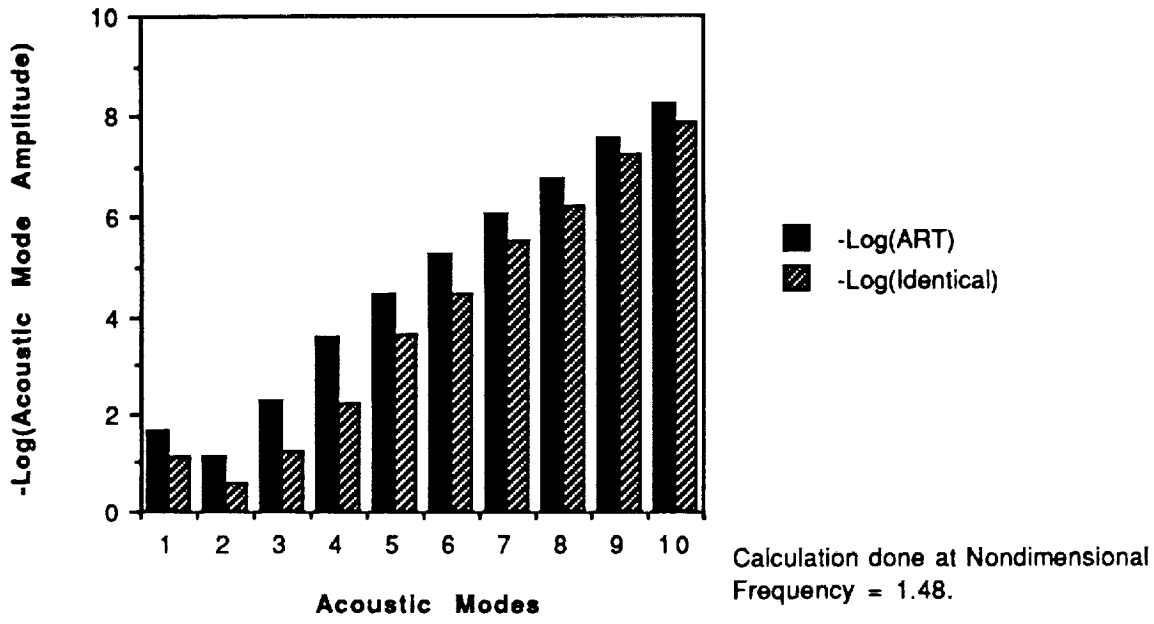

Figure 3b-9: Relative comparison of first 10 modal contributions to noise reduction in the sweeping problem. Sweep speed is 20% below Mach 1.

Section 3c: Panel-Frame Methodology

A copy of the paper entitled "Analysis of Sound Transmission Through Flexible Panel/Frame Walls," by D. B. Bliss, has been appended to the end of this report.

Section 3d: High Frequency ART

A copy of the paper entitled "High Frequency Alternate Resonance Tuning," by D. B. Bliss and R. Srinivasan, has been appended to the end of this report.

SECTION 4. EXPERIMENTAL VERIFICATION

Experimental verification continues with the Alternate Resonance Tuning concept. This section highlights the current experimental work. The various topics described below are presently at different stages of completion. These topics include the following:

- experimental verification of the ART concept using real panel sections

- experimental verification of the ART concept under simulated propagating external pressure fields in a 2-D environment.

Section 4a: Experimental Investigation of Real Panel Tuning Using the ART Methodology

Initial work has been completed on testing real panel sections to determine if the ART effect can be achieved. Figure 4a-1 shows the typical experimental setup used. A pure tone generator is driven mechanically through a frequency range of interest; two microphones are used to measure the upstream sound level (nearest the sound source) and the downstream level (beyond the panel wall) in the duct in dB . The AC microphone signals are high pass filtered and rectified to a DC signal proportional to the sound pressure level of the signals. Using LabVIEW, these signals are measured and converted to dB, and then written to the hard disk as a file with frequency and the two microphone levels, as well as the difference between the two microphone levels. LabVIEW then plots the noise reduction across the panel barrier; additionally, all data is saved and may be retrieved for later analysis and plotting. This system has proven extremely simple and reliable to use; furthermore, it is a versatile system which can be calibrated for use through many frequency ranges and sound pressure levels. Adjustment of the computer sampling interval effectively changes the bandwidth of the instrument. Additionally, a Scientific Atlanta SD-380 spectrum analyzer is used to verify the panel noise

reduction data using a transfer function option with a white noise input substituted for the pure tone generator. Unfortunately, the Acoustics Laboratory does not have available yet the Macintosh/SD-380 interface; therefore, since no data transfer is possible between the SD-380 and the Macintosh, the spectrum analyzer can only be used to verify the LabVIEW data results.

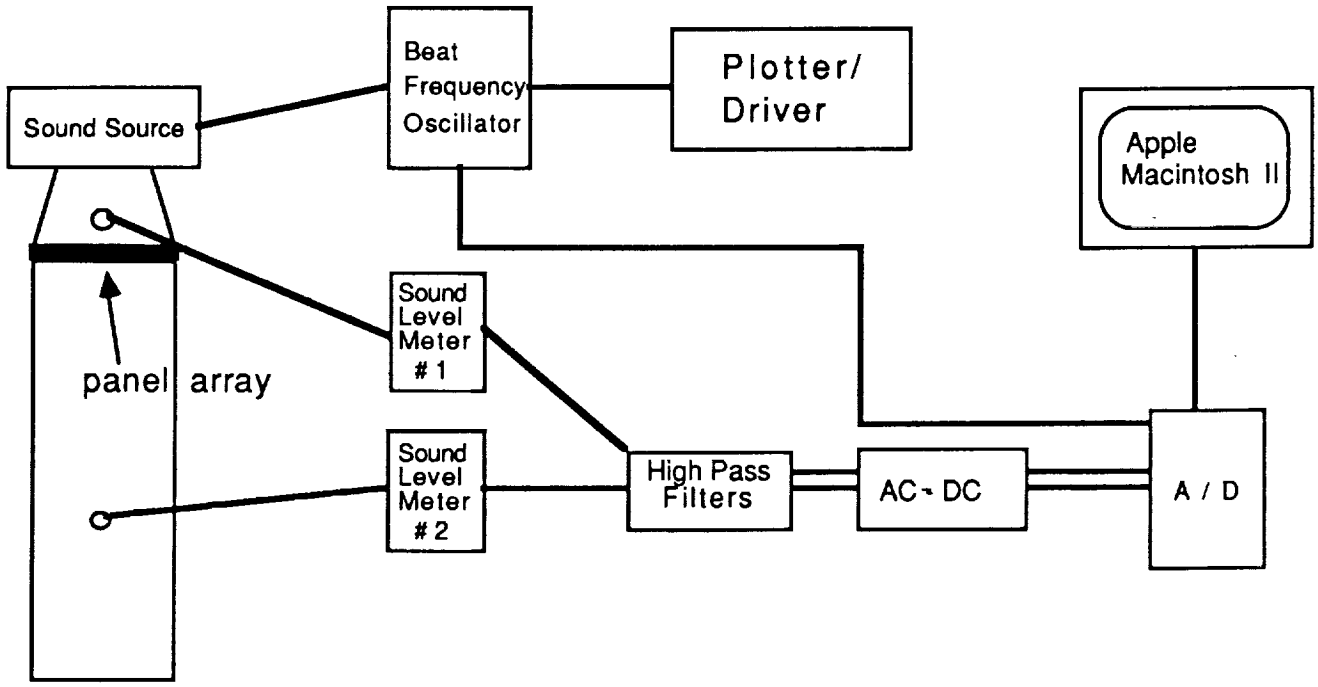

Figure 4a-1: Data acquisition setup for real panel experiment.

The actual panel setup is shown in Figure 4a-2. The apparatus consists of two pieces of rectangular aluminum frame with overall inside duct size 8" by 4". Two openings are cut into the frame for panel support; each panel measures 4" by 3-7/8". 27 socket head screws are used to clamp the two sections together around a set of Bakelite panels. For the most effective clamping, it is best if both panels are of the same material thickness. Future modifications may consider panels of differing thickness if the boundary condition can be

effectively implemented. It must be pointed out that the performance of the panels in the duct is highly dependent on the boundary conditions. Initial efforts to "shim" thinner panels along side thicker panels yielded unrealistic results.

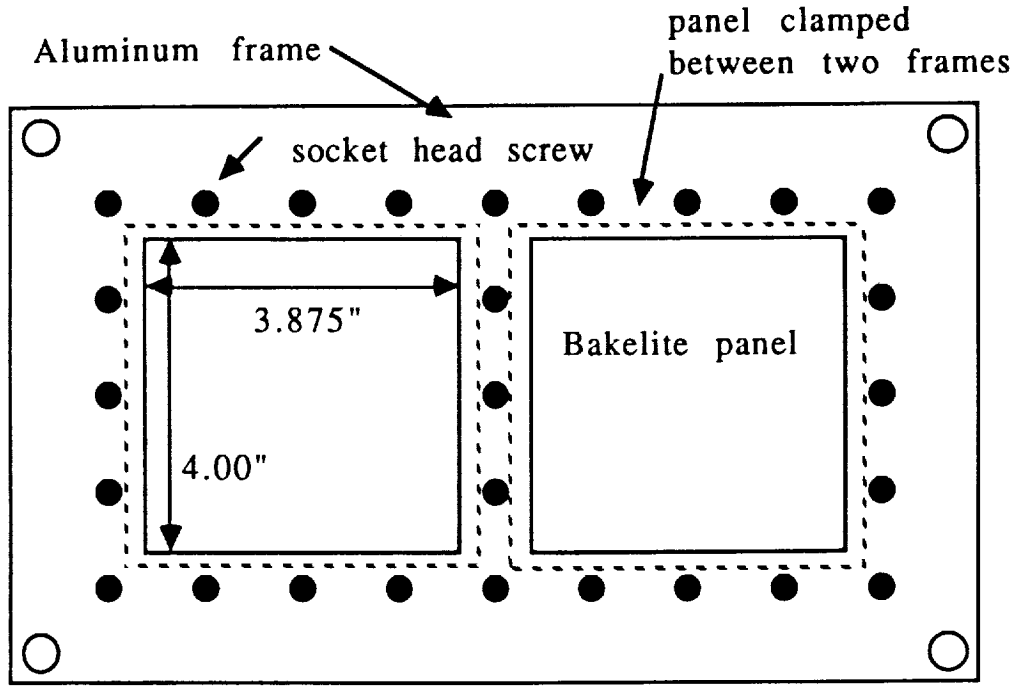

Figure 4a-2: Experimental panel holder for ART real panel test

Preliminary measurements were made using a single 4" by 4" duct along with the data acquisition setup. Figure 4a-3 shows the noise reduction measured across a Bakelite panel 1/64" thick, measuring 4" by 3-7/8". The boundary condition is clamped. At lower frequencies, behavior resembles typical stiffness dominated behavior, showing a noise reduction drop of approximately 6 dB/octave. The low frequency irregularities are most probably due to the termination impedance; it is not perfectly anechoic, especially at lower frequencies. Irregularities are also seen in the high frequency range due perhaps to duct resonances or other unknown effects. A noise reduction minimum is observed at approximately 475 Hertz, corresponding to the panel natural frequency.

In order to achieve the ART effect, a small amount of mass was added to the center of a similar 1/64" Bakelite panel. The noise reduction data for this panel with mass addition in the single panel duct is shown in Figure 4a-4. The first noise reduction minimum has dropped to 315 Hertz as a result of mass addition; a second noise reduction minimum is observed at 830 Hertz.

It is useful to compare the experimental data with plate theory to determine just how predictable the panel behavior is. As mentioned earlier, panel noise reduction behavior has been observed in the laboratory to be highly dependent on the boundary conditions. For example, the data shown in Figures 4a-3 and 4a-4 cannot be easily duplicated if the panel is not firmly attached and evenly seated in the frame. Any foreign matter interfering in the panel/frame interface can cause anomalies in the data. For the case of Figure 4a-3, however, the comparison between theory and data is quite good. For a square plate with four clamped boundary conditions, the natural frequencies are given by*

$$\omega_i = \frac{\lambda_i}{b^2}\sqrt{\frac{D}{m}} \qquad (4a\text{-}1)$$

where b is the length of a side of the plate. D is the flexural rigidity, denoted by

$$D = \frac{Eh^3}{1 - \nu^2} \qquad (4a\text{-}2)$$

where E is Young's modulus, h is the plate thickness, m is the mass per unit area of the plate, and ν is Poisson's ratio. For Bakelite, ν was assumed to be 0.3. λ_i are the solutions of the eigenvalue problem, and are shown below for the first three natural frequencies, along with other important values.

b	4 inches
E	0.6 - 1.0 x 10^{10} Pa
m	0.516 kg/m^2 for 1/64" panel

* See, for example, Szilard, R., *Theory and Analysis of Plates Classical and Numerical Methods*, Prentice-Hall, Inc., Englewood Cliffs, New Jersey, 1974.

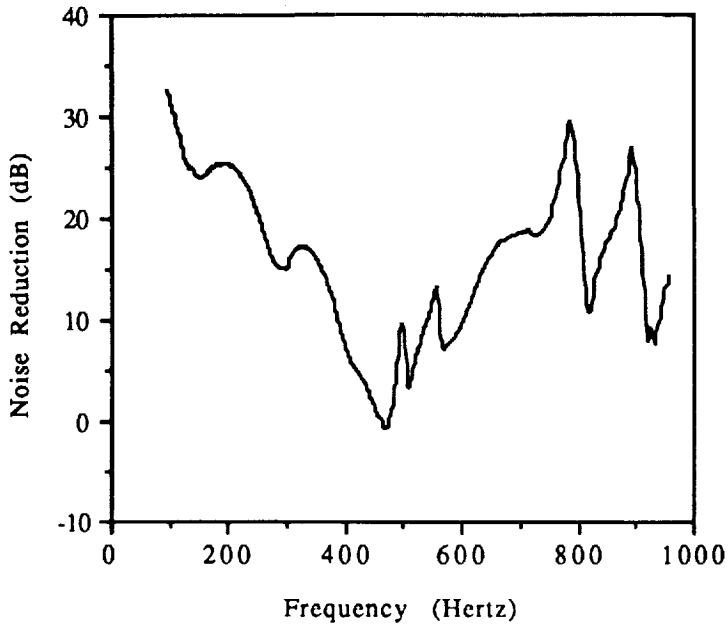

Figure 4a-3: Single 1/64" Bakelite panel in the single panel duct. No mass is added to this panel.

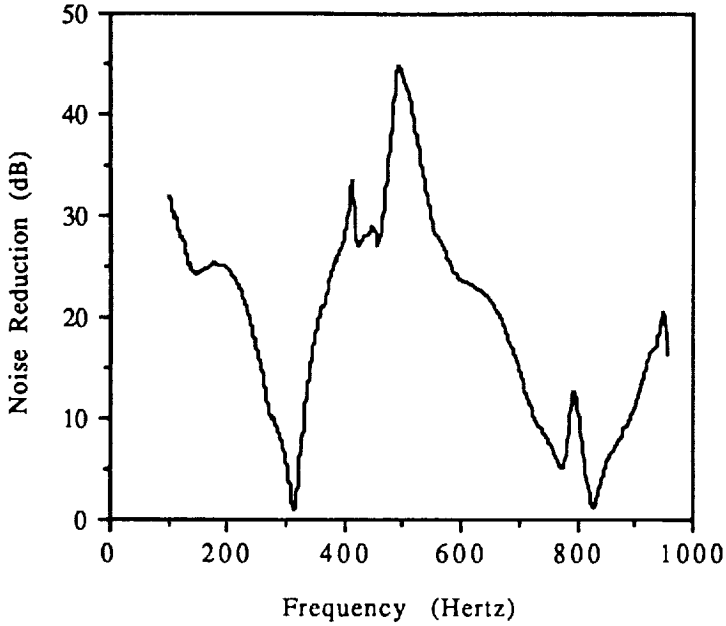

Figure 4a-4: Noise reduction for a single 1/64" Bakelite panel with mass added at panel center in the single panel duct.

$\lambda 1$	36.0
$\lambda 2$	73.8
$\lambda 3$	109.0

Substitution of pertinent data into 4a-2 yields a first mode natural frequency of 496 Hertz, very close to the data shown in Figure 4a-3, where a natural frequency of 475 Hertz was indicated.

However, the addition of a point mass to the 1/64" Bakelite panel causes the panel behavior to be different than that which could be predicted by Equation 4a-1. It is curious to note the ratio of the two frequencies corresponding to the noise reduction minima; i.e.,

$$\frac{\omega_1}{\omega_2} = \frac{830}{315} \cong 2.5$$

This ratio is similar to the ratio of natural frequencies for $\omega 11$ and $\omega 12$ for a pinned plate. Again from Szilard, for a square plate with pinned boundaries on 4 sides,

$$\omega_{mn} = \pi^2 \left[\frac{m^2}{b^2} + \frac{n^2}{b^2} \right] \sqrt{\frac{D}{m}} \qquad (4a\text{-}3)$$

Plugging in m=1 and n=1 for $\omega 11$, m=1 and n=2 for $\omega 12$, we can solve for a ratio of natural frequencies as

$$\frac{\omega_{12}}{\omega_{11}} = \frac{1^2 + 2^2}{1^2 + 1^2} = 2.5 \qquad (4a\text{-}4)$$

Arguably, the panel with additional mass may behave more like a pinned panel, according to plate theory equations. However, the presence of this second mode has created an amazing noise reduction between the two natural frequencies; a reduction in the transmitted noise of about 44 dB is seen at just below 500 Hertz. Remember that this is for a single panel in a single panel duct. It may therefore be possible to use higher structural mode behavior to some advantage in

ART tuning a real panel. Also, the point mass placed at the center of the panel may help to enforce higher structural mode vibration.

Figure 4a-5 shows the noise reduction data for both the 1/64" panel with no added mass and the 1/64" panel with added mass alongside each other, clamped in the two panel duct. The noise reduction minimum at 315 Hertz corresponds to the natural frequency of the panel with added mass; the noise reduction minimum at 475 Hertz corresponds to the ω_{11} natural frequency of the panel with no added mass, and an ART noise reduction effect of about 40 dB is observed at 350 Hertz. Similarly, the minima at 800 Hertz might correspond to the ω_{12} natural frequency of the panel with no added mass, and another ART noise reduction peak of 44 dB is observed at about 660 Hertz. If the panel with no added mass is actually behaving with two structural resonance frequencies, then the observed behavior shows two noise reduction minima as a result of three panel natural frequencies, as the ART theory has suggested.* Figure 4a-6 shows all 3 data sets on the same plot for comparison purposes.

A second experiment was conducted with 1/16" Bakelite panels, following the same procedure as above. Figure 4a-7 shows the noise reduction across a 1/16" Bakelite panel in a single panel duct. Here at lower frequencies, we again see approximately a 6 dB rolloff of the noise reduction due to stiffness dominated behavior. The panel resonance frequency appears to be at about 585 Hertz for this panel. Figure 4a-8 shows the noise reduction across a 1/16" Bakelite panel in the single panel duct with mass added in the panel center, effectively lowering the resonance frequency to about 430 Hertz. Due to a thicker and stiffer panel section, addition of more mass (compared to the 1/64" panels) resulted in less reduction of the panel resonance frequency. Both panels combined in the double panel duct produces the data shown in Figure 4a-9. Noise reduction minima are observed at 440 Hertz and 600 Hertz; however, the thicker panel combinations yield larger noise reductions at the panel natural frequencies; presumably due to a slightly greater damping, these panels appear

---

* D. B. Bliss and J. A. Gottwald, "Reduction of Sound Transmission Through Fuselage Walls by Alternate Resonance Tuning (ART)", accepted for publication in the AIAA *Journal of Aircraft*, in final revision.

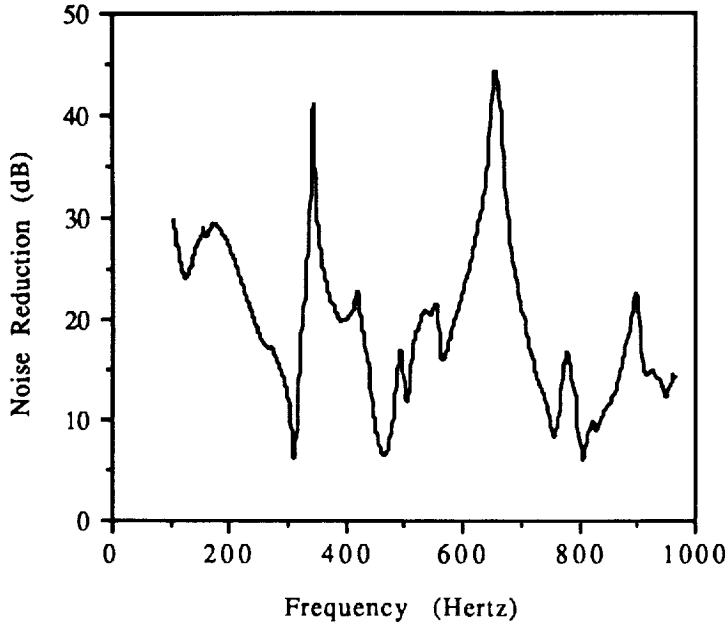

Figure 4a-5: Two panel ART result with two Bakelite panels in the duct.

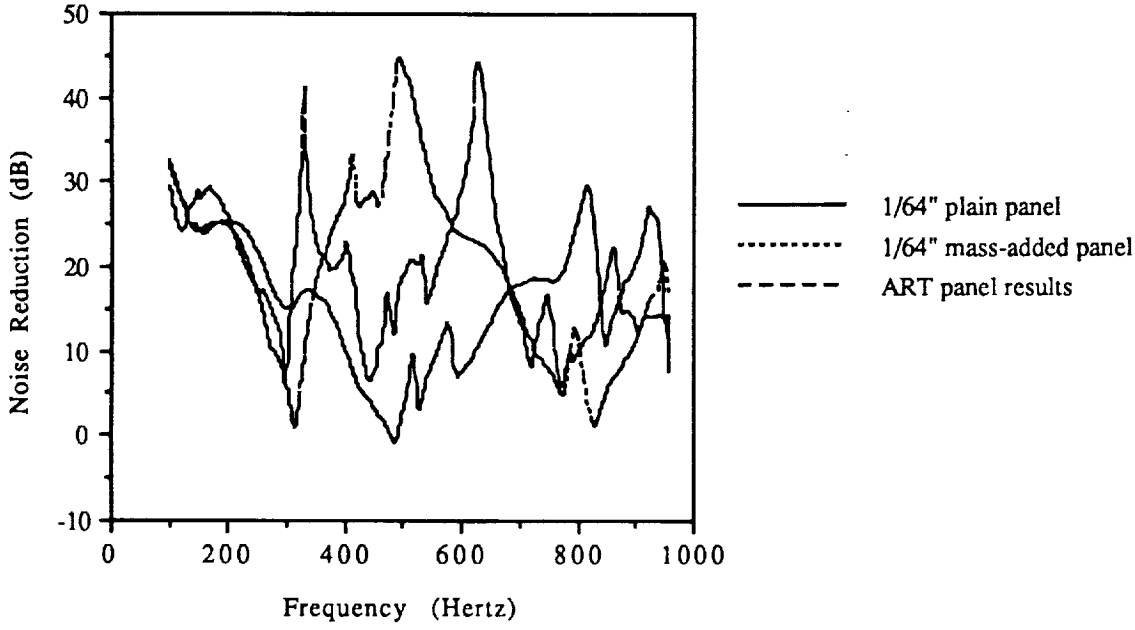

Figure 4a-6: Noise reduction results for all 1/64" Bakelite panel measurements.

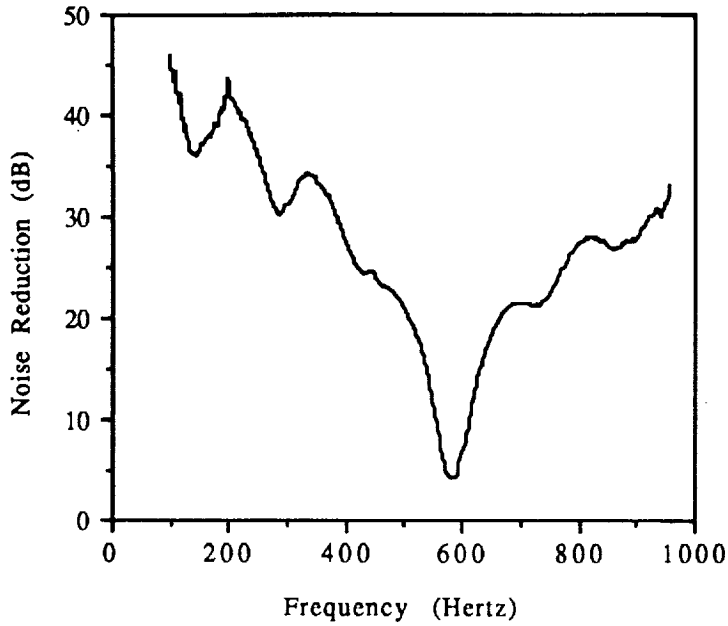

Figure 4a-7: Noise reduction across 1/16" Bakelite panel with no added mass.

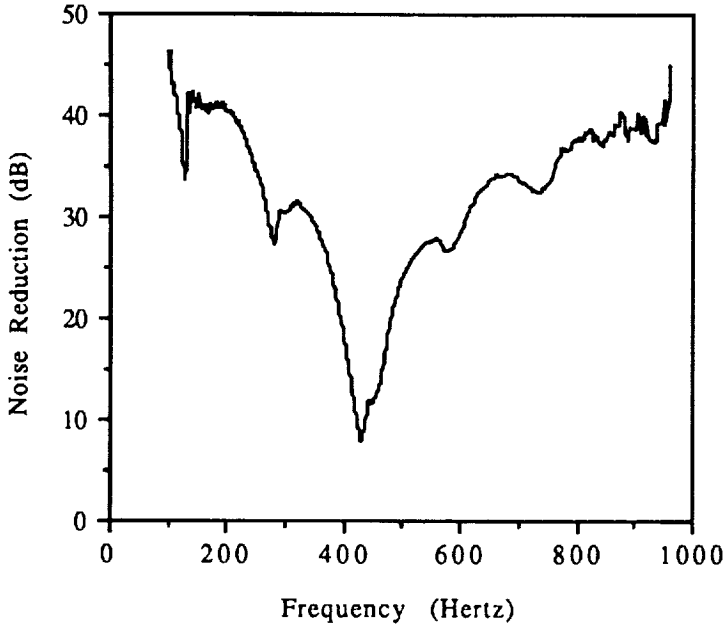

Figure 4a-8: Noise reduction across 1/16" Bakelite panel with added mass.

less transparent at the structural resonances. Finally, Figure 4a-10 shows all 3 data sets on one plot.

Less can be clearly inferred from the thicker panel noise reduction data with respect to the plate theory. In fact, Equation 4a-1 would indicate a first mode natural frequency at about 2000 Hertz for a plain 1/16" clamped plate. However, for the pinned theory, Equation 4a-3 indicates ω_{10} as 544 Hertz (a short search through relevant literature did not indicate if in fact this mode can exist!), and ω_{11} as 1088 Hertz. ω_{12} is much higher at 2720 Hertz, out of the current frequency range of interest.

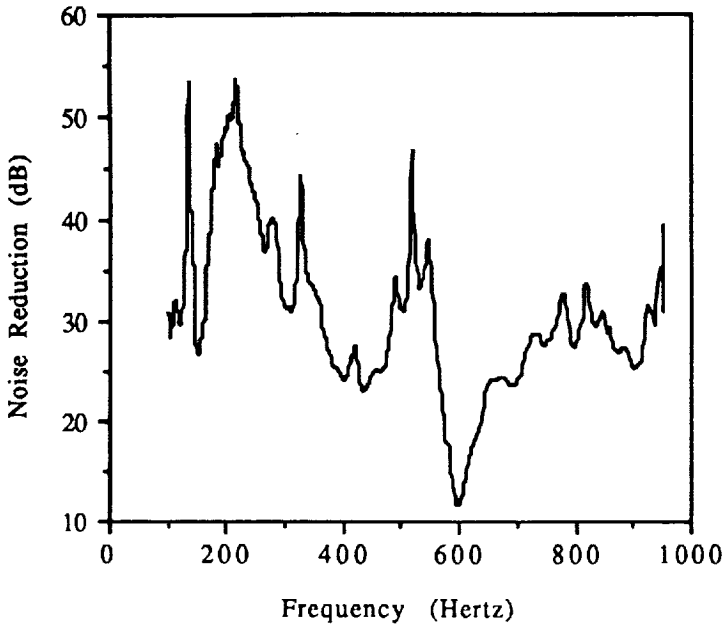

Figure 4a-9: Noise reduction across two 1/16" Bakelite panels in the two panel duct. Note ART cancellation between 430 Hz and 600 Hz.

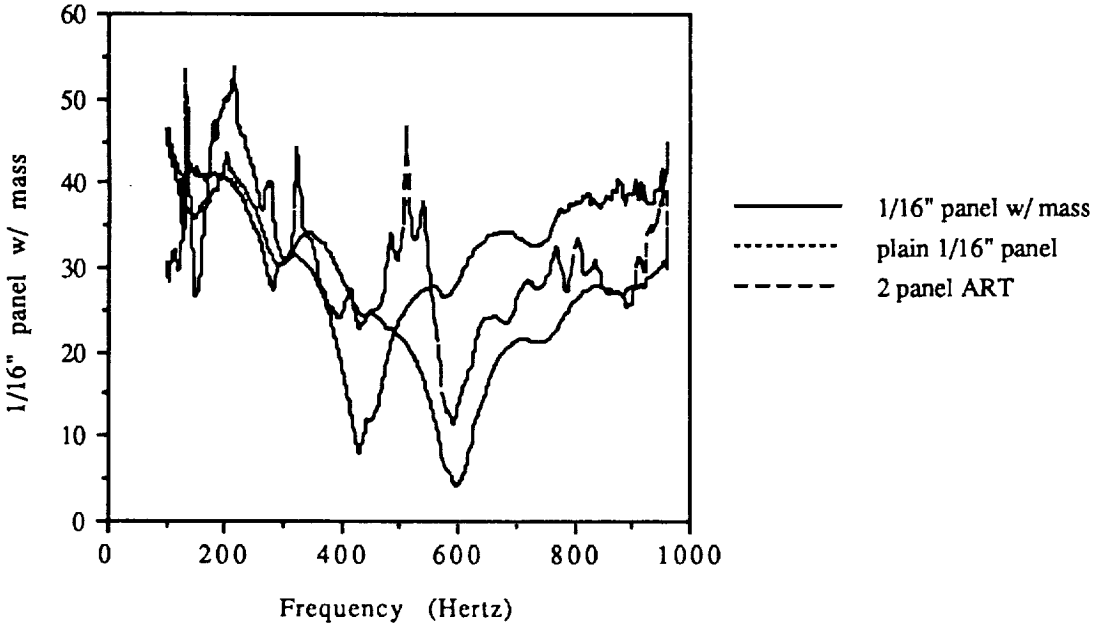

Figure 4a-10: 1/16" Bakelite panel results.

SECTION 5. FUTURE EFFORT

The planned path for the next six month period centers on continuing the development of realistic panel wall models incorporating the ART concept and use of the model to predict noise transmission through a paneled structure. This research will be carried out using the following approaches:

1) Development of the real panel computational code.

This work will be carried out first using a version of the branch analysis. The computer code will include higher structural modes from Equation 3a-24, but not higher acoustic modes, since previous work has indicated that these higher acoustic modes play a lesser role in the general panel behavior. It is hoped that an analytic expression for the transmitted pressure can be obtained as a function of the number of structural modes. Also, it may be possible to obtain closed-form results for a simpler geometry with additional acoustic modes; i.e., the two-panel problem.

2) Development of the corresponding double wall model.

3) More development on related model problems.

4) More parametric studies with existing models.

5) More development on the panel frame theory.

6) More experimental verification of the ART concept.

In particular, the behavior of the higher structural modes will be examined in greater detail. Most probably, thinner plates will be used since these seem to yield interesting results and effect ART-like behavior resulting from the higher modes.